EXOTIC BARYONS

L.G. Landsberg

IHEP, Protvino, Russia[1]

1. Introduction

A rapid development of the hadron spectroscopy in recent years has led to a significant advance in the systematics of "ordinary" hadrons with the simplest valence quark structure: $q\bar{q}$ for mesons and qqq for baryons. At the same time several unusual hadrons with some anomalous features have been found. They do not fit in the systematics of this simplest quark model and are interpreted as a new form of hadronic matter – exotic hadrons. These states can include multiquark formations ($qq\bar{q}\bar{q}$ mesons and $qqqq\bar{q}$ baryons), hybrid systems with valence quarks and gluons ($q\bar{q}g$ mesons and $qqqg$ baryons), or glueballs, i.e. mesons consisting solely of valence gluons (gg, ggg). The discovery of the exotic hadrons would have far-reaching consequences for quantum chromodynamics, for the concept of confinement and for specific models of hadron structure (lattice, string and bag models). Detailed discussions of exotic hadron physics can be found in recent reviews [1-7].

Exotic hadrons can have anomalous quantum numbers not accessible to three-quark baryons or quark-antiquark mesons (open exotic states), or even usual quantum numbers (cryptoexotic states). Cryptoexotic hadrons can be identified only by their unexpected dynamical properties (anomalously narrow decay widths, anomalous decay branching ratios and so on).

As is clear from review papers [1-7], in the last decade searches for exotic mesons have led to considerable advances in this field. Several new states have been observed whose properties cannot be explained in the framework of naive quark model of ordinary mesons with $q\bar{q}$ valence quark structure. These states are serious candidates for exotic mesons (most of them are of cryptoexotic type).

At the same time the situation for exotic baryons is far from being clear. There are also some examples of possible unusual baryon resonances [8-11], but these data are not sufficiently precise and are not supported by some new experimental results [2,12-16].

Extensive studies of the diffractive baryon production and search for cryptoexotic pentaquark baryons with hidden strangeness ($B_\phi = |qqqs\bar{s}>$, here $q = u, d$ quarks)

---

[1]The SPHINX Collaboration (IHEP-ITEF):
V.A. Bezzubov, S.V. Golovkin, A.P. Kozhevnikov, V.P. Kubarovsky, A.I. Kulyavtzev, V.F. Kurshetsov, L.G. Landsberg, V.V. Molchanov, V.A. Mukhin, I.N. Nikitin, V.I. Solyanik, D.V. Vavilov, V.A. Victorov (Institite for High Energy Physics. Protvino, Russia); M.Ya. Balatz, G.V. Dzubenko, G.K. Kliger, V.Z. Kolganov, G.S. Lomkatzi, A.F. Nilov, V.T. Smolyankin, V.E. Vishnyakov (Institute of Theoretical and Experimental Physics, Moscow, Russia).

are being carried out by the SPHINX Collaboration at the IHEP accelerator with 70 GeV proton beam. This program was described in detail in reviews [2].

The recent data of the SPHINX experiment [16-21] gave new important evidence of possible existence of cryptoexotic baryons with hidden strangeness $X(2050)^+ \to \Sigma(1385)^0 K^+$ and $X(2000)^+ \to \Sigma^0 K^+$. We shall summarize these data in Sections 3-6, after a general description of the nature and expected properties of cryptoexotic baryons, as well as some promising ways for their production and observation. We shall also present here first data on the $\Sigma^0\pi^0$ system and on possible new effects in different proton diffractive-like processes in a nonperipheral domain. Some earlier results obtained in the first measurements with the SPHINX spectrometer were published in [12-16,22]. We don't discuss them here.

2. Cryptoexotic baryons

As has been stated before, cryptoexotic baryons do not have external exotic quantum numbers and their complicated internal valence structure can be established only indirectly, by examination of their unusual dynamic properties which are quite different from those for ordinary $|qqq>$ baryons. In this connection let us consider the properties of multiquark baryons with hidden strangeness $B_\phi = |qqqs\bar{s}>$ $(q = u, d)$.

If such cryptoexotic baryon structure consists of two color parts separated in space with a centrifugal barrier, then its decays into the color singlet final states may be suppressed because of a complicated quark rearrangement in decay processes. The properties of multiquark exotic baryons with internal color structure

$$|qqqq\bar{q}>_{1c} = |(qqq)_{8c} \bigodot (q\bar{q})_{8c}> \quad (1)$$

(color octet bonds) or

$$|qqqq\bar{q}>_{1c} = |(qq\bar{q})_{\bar{6}c} \bigodot (qq)_{6c}> \quad (2)$$

(color sextet-antisextet bonds) are discussed in [23-25]. Here subscripts 1c, 8c and so on specify the representation of the color SU$(3)_c$ group. If the mass of a nonstrange baryon with hidden strangeness is above the threshold for the decay modes with the strange particles in final states, then the main decay channels should be of the type

$$B_\phi \to YK + n\pi \quad (3)$$

(n=0;1;...). Another possibility is associated with the decays

$$B_\phi \to \phi N(\eta N; \eta' N) + n\pi, \quad (4)$$

i.e. with emission of particles with a significant $s\bar{s}$ component in their valence quark structure. It must be also stressed that η and particularly η' mesons are strongly coupled with gluon fields and, then, with states with enriched gluon component. Therefore baryon decays of $B \to N\eta, N\eta'$ type may be the specific decay modes for the hybrid baryons (see, for example, reviews [2]).

The nonstrange decays of baryons with hidden strangeness $B_\phi \to N + n\pi$ must be suppressed by the OZI rule. Thus, the effective phase space factors for the decays of massive B_ϕ baryons would be significantly reduced because of this OZI suppression (owing to a large enough mass threshold for the allowed $B_\phi \to YK$ decays to be compared with suppressed $B_\phi \to N\pi$, $\Delta\pi$ ones). The mechanism of quark rearrangement of color clusters in the decay processes for the objects with complicated inner structure of (1) or (2) type can additionally reduces the decay width of cryptoexotic baryons and makes it anomalously narrow (of the order of several tens of MeV). The theoretical predictions here are rather arbitrary. So the question of the existence of such narrow baryon resonances with hidden strangeness can be resolved only experimentally.

Thus, it seems quite desirable to perform the systematical search for cryptoexotic baryons B_ϕ with anomalous dynamical features which are listed below:

1. The dominant OZI allowed decay modes of B_ϕ baryons are the ones with strange particles in the final states (for ordinary baryons such decays have branching ratios at the percent level).

2. Cryptoexotic B_ϕ baryons can possess both a large mass (M $> 1.8 \div 2.0\,\mathrm{GeV}$) and a narrow decay width ($\Gamma \leq 50 \div 100\,\mathrm{MeV}$). This is due to a complicated internal color structure of these baryons with significant quark rearrangement of color clusters in the decay processes and due to a limited phase space for the OZI allowed $B \to YK$ decays. At the same time typical decay widths of the well established $|qqq>$ isobars with similar masses are $\geq 300\,\mathrm{MeV}$.

As was emphasized in a number of papers [1,2,8,10,24,26,27], diffractive production processes with Pomeron exchange offer new tools in searches for the exotic hadrons. Originally, the interest was concentrated on the model of Pomeron with small cryptoexotic ($qq\bar{q}\bar{q}$) component [24,26]. In modern notions Pomeron is a multigluon system which allows for production of the exotic hadrons in gluon-rich diffractive processes (see Fig.1).

The Pomeron exchange mechanism in diffractive production reactions can induce the coherent processes on the target nucleus. In such processes the nucleus acts as a whole. Coherent processes can be easily identified by the transverse momentum spectra of the final state particle systems. They manifest themselves as diffractive peaks with large values of the slope parameters determined by the size of the nucleus: $\mathrm{d}N/\mathrm{d}P_\mathrm{T}^2 \simeq \exp(-bP_\mathrm{T}^2)$, where $b \simeq (8{\div}10)A^{2/3}\,\mathrm{GeV}^{-2}$. Owing to the difference in the absorption of single-particle and multiparticle objects in nuclei, coherent processes could serve as an effective tool for the separation of resonance against non-resonant multiparticle background (see, e.g. Ref.[28]). This idea is illustrated schematically in Fig.2.

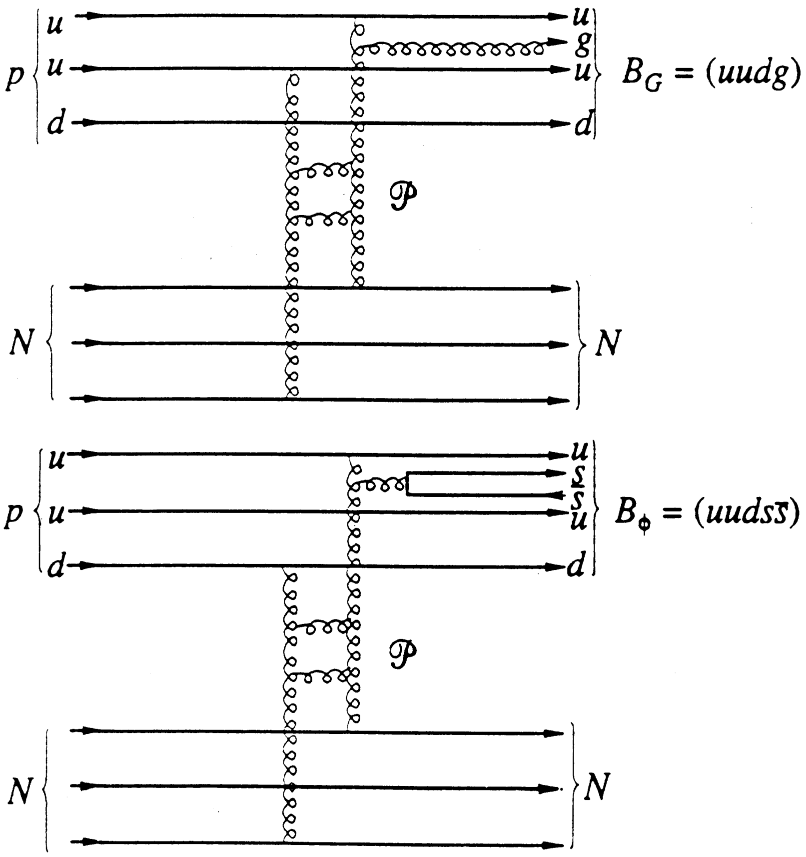

Figure 1: The diagrams for exotic baryon production in the diffractive processes with Pomeron exchange (gluon-rich processes).

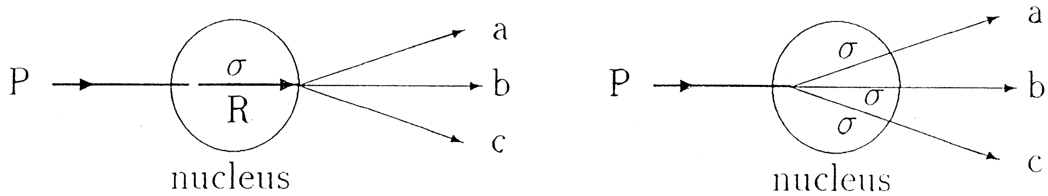

Figure 2: Schematic illustration of the coherent suppression of non-resonance multiparticle background in the reactions $p+$(Nucleus) $\to R+$(Nucleus), $R \to a+b+c$ (resonance production) and $p+$ (Nucleus) $\to [abc]+$ (Nucleus) (nonresonant background) due to a difference in the resonance and background absorption in the target nuclei. As a result of this coherent suppression of nonresonant background it is possible to obtain:
$\frac{\sigma_{\text{coh}}(\text{resonance})}{\sigma_{\text{coh}}(\text{background})} > \frac{\sigma_{\text{noncoh}}(\text{resonance})}{\sigma_{\text{noncoh}}(\text{background})}$.

3. The experiments with the SPHINX setup

A study of several proton-induced diffractive production processes of $p + N \to Y^0 K^+ + N$ type as well as $p + N \to pK^+K^- + N, p + N \to pp\bar{p} + N$, $p + N \to p\pi^+\pi^-\pi^0 + N$ and several other reactions was carried out by the SPHINX Collaboration in 70 GeV proton beam with a polyethylene target. The SPHINX detector used in these measurements includes a wide-aperture magnetic spectrometer with scintillator hodoscopes, proportional wire chambers, drift chambers and a multichannel γ-spectrometer made of total absorption lead glass detectors. Charged particles of the final state were identified with differential RICH spectrometer and two multicell gas threshold Cherenkov counters $\breve{C}_1$ and $\breve{C}_2$. The layout of the SPHINX setup is presented in Fig.3. A detailed description of the apparatus can be found in Ref.[12].

For the separation of different exclusive reactions a complete kinematic reconstruction of the events was used with the account of the information from tracking detectors, magnetic spectrometer, γ - spectrometer and all Cherenkov counters of the SPHINX setup. In the final stage of this reconstruction procedure the identification of the reactions under study was achieved by the examination of effective mass spectra for subsystems of secondary particles, as it is illustrated in Fig.4.

As is seen from dN/dP_T^2 spectra for above mentioned processes, there are strong narrow forward cones in these distributions with the slope $b \geq 40 - 50$ GeV^{-2} which correspond to a coherent diffractive production on carbon nuclei (Fig.5). For identification of the coherently produced events "loose" or "tight" cuts in P_T^2 can be used:

1. "loose" transverse momentum cut: $P_T^2 < 0.075 \div 0.1$ GeV^2; with this cut noncoherent background in event sample can be as large as 30-40%;

2. "tight" transverse momentum cut: $P_T^2 < 0.02$ GeV^2; with this cut noncoherent background is reduced to $< 8 - 10\%$ of the event sample at the cost of lower signal statistics.

   All diffractive and coherent reactions mentioned above were used for thorough searches for new baryon states, especially for candidates for cryptoexotic baryons with hidden strangeness [12-21]. But the most interesting results were obtained in a study of $\Sigma^*(1385)^0 K^+$ and $\Sigma^0 K^+$ systems produced in the coherent diffractive reactions on carbon nuclei

$$p + C \;\to\; [\Sigma(1385)^0 K^+] + C \qquad (5)$$
$$\hookrightarrow \Lambda\pi^0$$
$$\hookrightarrow p\pi^-$$

and

$$p + C \;\to\; [\Sigma^0 K^+] + C. \qquad (6)$$
$$\hookrightarrow \Lambda\gamma$$
$$\hookrightarrow p\pi^-$$

a.)

b.)

c.)

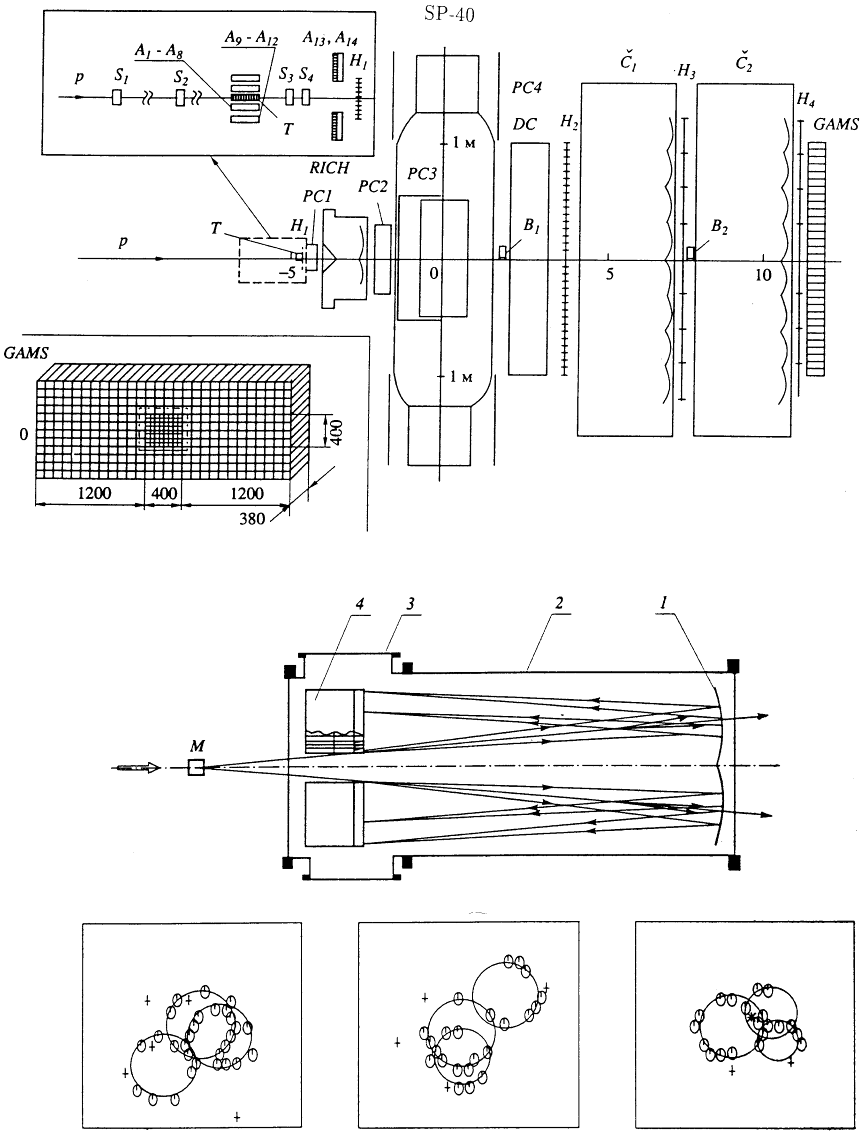

Figure 3: a) The layout of the SPHINX spectrometer. $S1-S4$, $B1$, $B2$ are scintillation counters, $A1-A14$ are scintillation guard counters, $H1-H4$ are scintillation hodoscopes; $PC1-PC4$ are blocks of proportional chambers; DC is the block of drift chambers; SP - 40 is a spectrometer magnet; $\breve{C}_1, \breve{C}_2$ are hodoscope threshold Cherenkov counters; RICH is a Cherenkov ring image spectrometer; GAMS is the hodoscope γ - spectrometer (which is presented on the left lower part of the figure; the dutt-dotted line indicates the active region of γ detector which is used for trigger requirement). b) The layout of Cherenkov RICH spectrometer with registration of the radiation rings: 1) - spherical mirror from the thin glass ($\Delta = 5\,\mathrm{mm}$, $f = 1250\,\mathrm{mm}$); 2) - the body of the counter; 3) - flanges; 4) - photomatrix with 736 phototubes FEU-60 with the photocathode 10 mm in diameter. c) The examples of the registrating Cherenkov radiation rings in photomatrix of the RICH spectrometer for the trigger events with 3 charged particles in the final state.

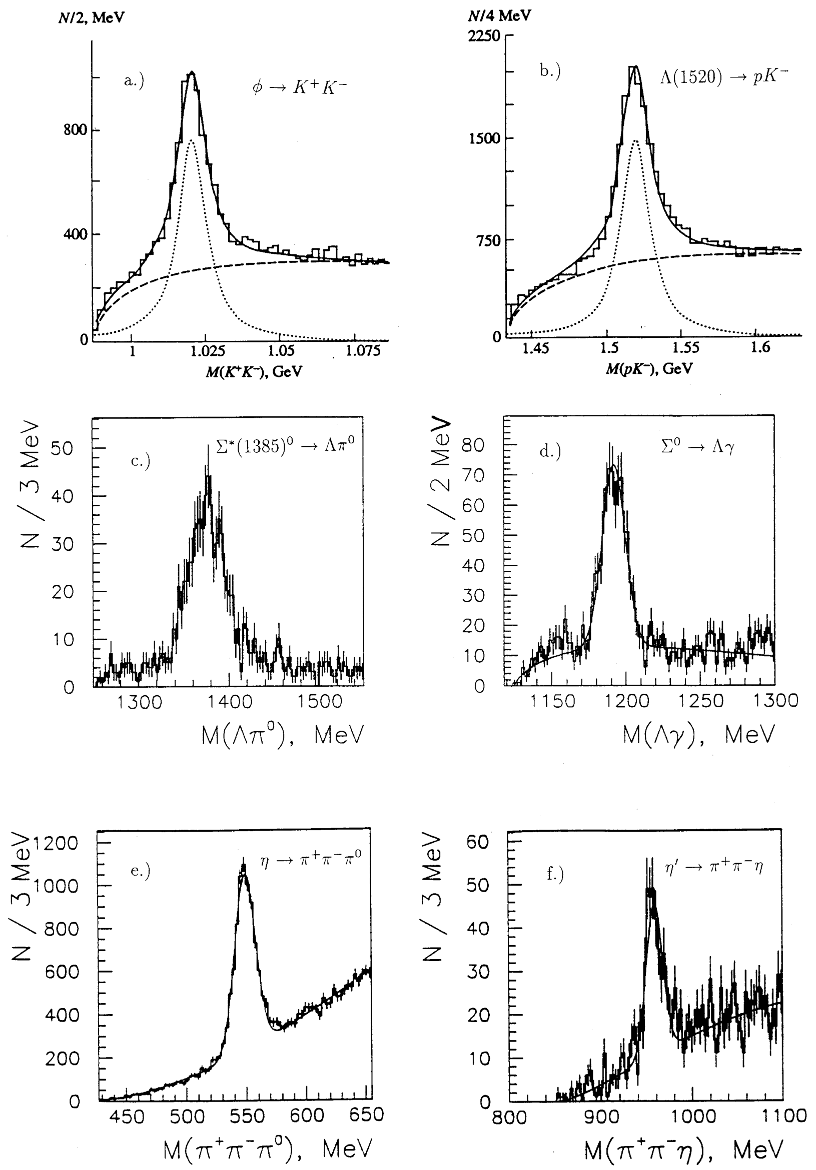

Figure 4: a, b) Selection of the reactions $p+N \to [p\phi]+N$ and $p+N \to [\Lambda(1520)K^+]+N$ from the invariant mass spectra $M(K^+K^-)$ and $M(pK^-)$ produced in the reaction $p+N \to [pK^+K^-]+N$.
c) Selection of the reaction $p+N \to [\Sigma^*(1385)^0K^+]+N$ from the invariant mass spectrum $\Lambda\pi^0$ produced in the reaction $p+N \to [\Lambda\pi^0K^+]+N$.
d) Selection of the reaction $p+N \to [\Sigma^0K^+]+N$ from the invariant mass spectrum of $(\Lambda\gamma)$ produced in the reaction $p+N \to [\Lambda\gamma K^+]+N$.
e) Selection of the reactions $p+N \to [p\eta]+N$ from the invariant mass spectrum $M(\pi^+\pi^-\pi^0)$ in $p+N \to [p\pi^+\pi^-\pi^0]+N$
f) Selection of the reaction $p+N \to [p\eta']+N$ from the invariant mass spectrum $M(\pi^+\pi^-\eta)$ in $p+N \to [p\pi^+\pi^-\eta]+N$.

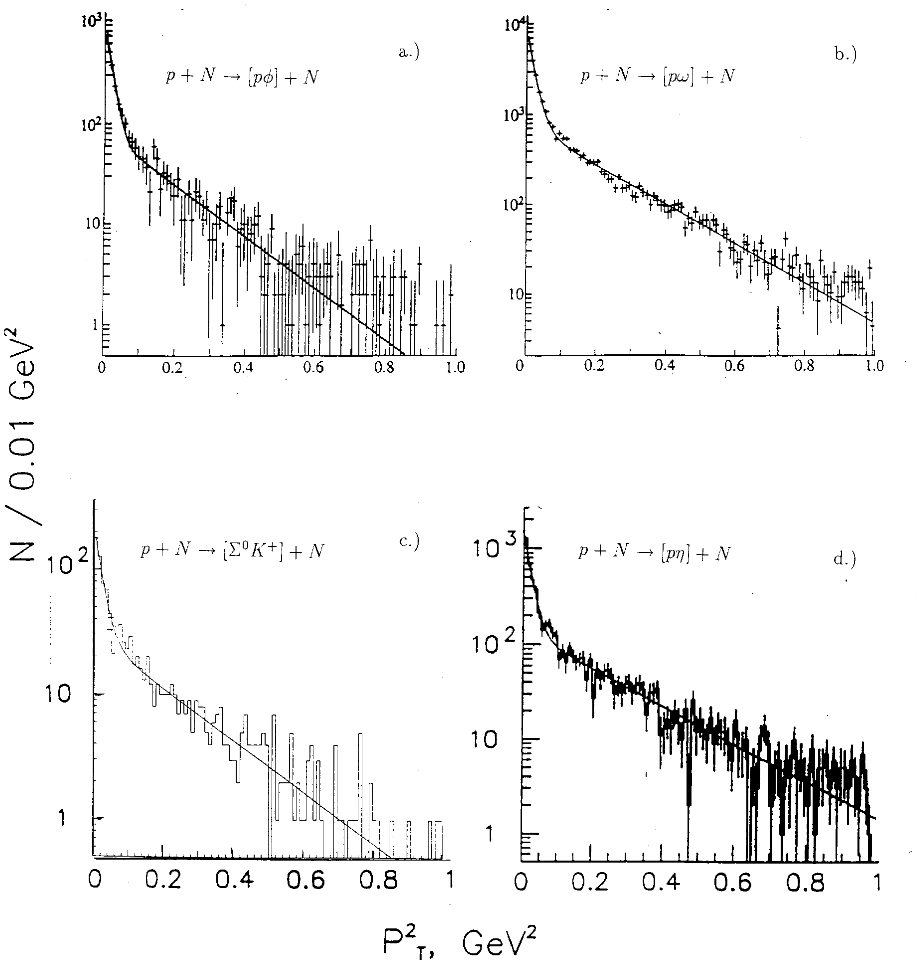

Figure 5: dN/dP_T^2 distributions for several reactions: a) for the reaction $p+N \to [p\phi]+N$; b) for the reaction $p+N \to [p\omega]+N$; c) for the reaction $p+N \to [\Sigma^0 K^+]+N$; d) for the reaction $p+N \to [p\eta]+N$. In all these distributions there are strong narrow forward cones with the slope $b \geq 40-50$ GeV^{-2}, which correspond to coherent diffractive production processes on carbon nuclei.

4. Previous data on the coherent diffractive reactions $p + C \to [\Sigma(1385)^0 K^+] + C$ and $p + C \to [\Sigma^0 K^+] + C$ [18-20]

4.1. Reaction $p + C \to [\Sigma(1385)^0 K^+] + C$

In the analysis of the SPHINX data the exclusive process with Λ hyperons $p + N \to [\Lambda\pi^0 K^+] + N$ was identified [13,14]. The invariant mass spectrum of the $\Lambda\pi^0$ system in this reaction is presented in Fig.4c. In the $M(\Lambda\pi^0)$ spectrum a peak corresponding to the $\Sigma(1385) \to \Lambda\pi^0$ decay is dominating. The background level under the $\Sigma(1385)^0$ peak is quite small. This fact simplifies the identification of reaction $p + N \to [\Sigma(1385)^0 K^+] + N$ and corresponding coherent reaction (5).

Coherent events of (5) were singled out in the analysis of dN/dP_T^2 distribution as a strong forward peak with the slope $b \sim 50$ GeV^{-2}. In order to reduce the non-coherent background and to obtain the $\Sigma(1385)^0 K^+$ mass spectrum for the "pure" coherent production reaction on carbon nuclei a "tight" requirement $P_T^2 < 0.02$ GeV^2 has been imposed and the mass spectra of $\Sigma(1385)^0 K^+$ for the coherent events of (5) have been obtained (see for example Fig.6). These spectra were studied with different values of ΔM bin widths in histograms and with bin shifting. The thorough background evaluation under the peaks was obtained using the information on the side bands near the peak. The statistical confidence levels of the peaks were determined from these data. See more details in [19].

The fits of the spectra with Breit – Wigner peaks and polynomial smooth background were carried out, and the average values for the main parameters of $X(2050)$ structure were determined:

$$\left.\begin{array}{l} M = 2052 \pm 6\,\mathrm{MeV}; \\ \Gamma = 35^{+22}_{-35}\,\mathrm{MeV} \\ \text{(with the account of the apparatus mass resolution);} \\ \text{statistical C.L. of the peak } \geq \text{ 5 standard deviations .} \end{array}\right\} \quad (7)$$

This narrow structure cannot be explained by diffractive nonresonant process of the Deck-type and seems to be caused by the production of a new cryptoexotic baryon with hidden strangeness.

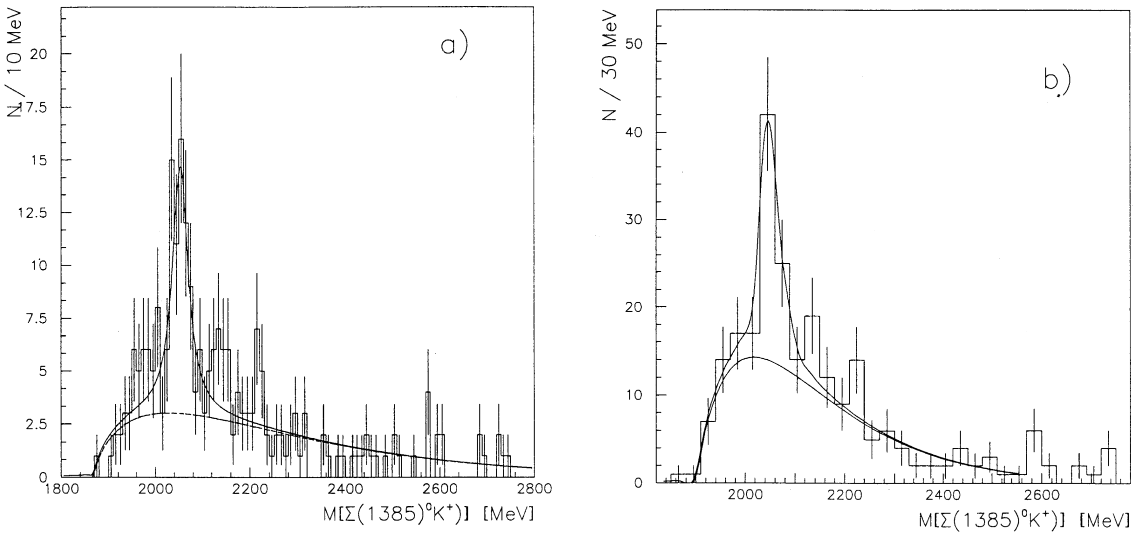

Figure 6: The invariant mass spectra $M[\Sigma^0(1385)K^+]$ in the coherent reaction (15) with tight transverse momentum cut $P_T^2 < 0.02$ GeV^2 and with different widths of bins: a) $\Delta M = 10$ MeV; b) $\Delta M = 30$ MeV. The spectra are fitted by the sum of smooth polynominal background curve and $X(2050)$ peak. The parameters of $X(2050)$ peak are: a) $M = 2053 \pm 4$ MeV, $\Gamma = 40 \pm 15$ MeV; b) $M = 2053 \pm 5$ MeV, $\Gamma = 35 \pm 16$ MeV.

4.2. Reaction $p + C \to [\Sigma^0 K^+] + C$

During the study of the reactions with Λ hyperons and K mesons the events with one and only one additional γ-cluster detected in γ-spectrometer of the SPHINX apparatus were separated.

Invariant mass spectrum of the $\Lambda\gamma$ system for these events is shown in Fig.4d. A peak corresponding to the $\Sigma^0 \to \Lambda\gamma$ decay is clearly seen in this spectrum, allowing for identification of reaction (6). Coherent events were selected using a P_T^2 cut.

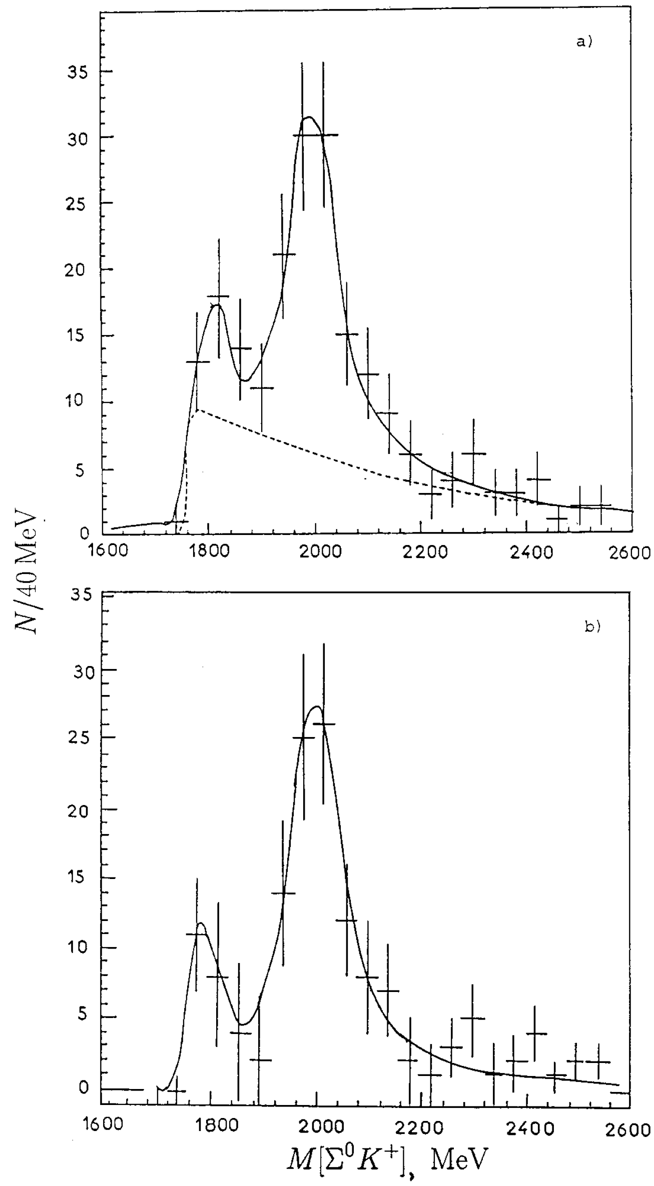

Figure 7: Invariant mass spectrum $M(\Sigma^0 K^+)$ in the coherent reaction (16) ($P_T^2 < 0.1$ GeV^2): a) - for all the events in the Σ^0 signal band in Fig.4d; b) - after sideband subtraction of the background under Σ^0 - peak in Fig.4d (old SPHINX data, see Ref. [19] for details).

Invariant mass spectrum $M(\Sigma^0 K^+)$ in the coherent reaction (6) for $P_T^2 < 0.1\mathrm{GeV}^2$ is shown in Fig.7. Apart from a small bump with $M \sim 1800$ MeV at the threshold, $X(2000)$-peak dominates the spectrum. The following parameters were measured for this peak:

$$\left.\begin{array}{l} M = 1997 \pm 7\,\mathrm{MeV}; \\ \Gamma = 91 \pm 17\,\mathrm{MeV}; \\ \text{statistical significance of the peak is 7 s.d.} \end{array}\right\} \tag{8}$$

Such a shape of the $\Sigma^0 K^+$ mass spectrum (with an additional structure at the threshold) proves that the $X(2000)$ peak can not be explained by a non-resonant Deck-type diffractive singularity. Therefore, this peak possibly has a resonant nature.

4.3. Study of Other Decay Channels for $X(2050)$ and $X(2000)$ States.

A search for other decay channels of the $X(2000)$ and $X(2050)$ baryon candidates was performed by analyzing data produced in the coherent reactions

$$p + C \;\rightarrow\; [p\pi^+\pi^-] + C \tag{9}$$

$$\rightarrow\; [\Delta(1232)^{++}\pi^-] + C. \tag{10}$$

These data were also collected by the SPHINX detector in kinematic conditions similar with (5) and (6). A preliminary analysis of the reaction with $[\Delta(1232)^{++}\pi^-]$ production was a subject of our earlier paper [13]. In this paper a diffractive production of two isobar-like structures with masses ≈ 1460 MeV and ≈ 1715 MeV was observed in the data. However, no peaks in 2 GeV mass range were observed in the mass spectra of $p\pi^+\pi^-$ and $\Delta(1232)^{++}\pi^-$ systems produced in reactions (9) and (10), respectively. Lower limits on the corresponding decay branching ratios were set to be (at the 95% C.L.):

$$\mathrm{R}_1 = \frac{\mathrm{BR}\{X(2050)^+ \to [\Sigma(1385)K]^+\}}{\mathrm{BR}\{X(2050)^+ \to [\Delta(1232)\pi]^+\}} > 1.7, \tag{11}$$

$$\mathrm{R}_2 = \frac{\mathrm{BR}\{X(2050)^+ \to [\Sigma(1385)K]^+\}}{\mathrm{BR}\{X(2050)^+ \to p\pi^+\pi^-\}} > 2.6, \tag{12}$$

$$\mathrm{R}_2' = \frac{\mathrm{BR}\{X(2050)^+ \to \Sigma(1385)^0 K^+\}}{\mathrm{BR}\{X(2050)^+ \to p\pi^+\pi^-\}} > 0.86, \tag{13}$$

$$\mathrm{R}_3 = \frac{\mathrm{BR}\{X(2000)^+ \to [\Sigma K]^+\}}{\mathrm{BR}\{X(2000)^+ \to [\Delta(1232)\pi]^+\}} > 0.83, \tag{14}$$

$$\mathrm{R}_4 = \frac{\mathrm{BR}\{X(2000)^+ \to [\Sigma K]^+\}}{\mathrm{BR}\{X(2000)^+ \to p\pi^+\pi^-\}} > 7.8, \tag{15}$$

$$\mathrm{R}_4' = \frac{\mathrm{BR}\{X(2000)^+ \to \Sigma^0 K^+\}}{\mathrm{BR}\{X(2000)^+ \to p\pi^+\pi^-\}} > 2.6. \tag{16}$$

Isotopic relations between the decay amplitudes of $I = \frac{1}{2}$ particles were assumed in these calculations ($X(2000)$ and $X(2050)$ states belong to isodoublets since they are produced in a diffractive dissociation of a proton).

Ratios $R_1 \div R_4$ of the widths of the $X(2000)$ and $X(2050)$ decays into strange and nonstrange particles are much larger than those for ordinary (qqq)-isobars [2,18].

Narrow widths of the $X(2000)$ and $X(2050)$ baryon states as well as anomalously large branching ratios for their decay channels with strange particles emission (large values of $R_1 \div R_4$) are the reasons to consider these states as serious candidates for cryptoexotic baryons with a hidden strangeness ($|uuds\bar{s}>$). At the existing level of statistics for reactions (5) and (6), as well as with possible background uncertainties the above results and conclusions must be considered as preliminary. They should be confirmed in further measurements with greatly increased statistics.

The problem of possible connection between the $X(2050)$ baryon state observed in reaction (5) and the $X(2000)$ baryon state observed in reaction (6) seems to be quite interesting. At a first sight the difference in their parameters (7) and (8) is significant. But to obtain the ultimate answer on the existence of two different baryonic states or only one state with two different decay channels we need to perform a further study of reactions (5) and (6) with increased statistics. It would give a possibility to obtain more precise information about the shape of these peaks, their decay widths and quantum numbers and to clear up a possible connection between these two structures.

Some new data on reaction (6) obtained with a partially upgraded SPHINX setup will be discussed below.

5. SPHINX detector upgrade

The SPHINX detector is undergoing a complete upgrade. It includes a new tracking system with proportional wire chambers and drift tubes, a new γ-spectrometer, new electronics, trigger systems, DAQ, and on-line computers. When this modernization will be finished, the SPHINX apparatus will have a possibility to work with higher luminosity and with significantly increased number of recorded triggers per accelerator burst (2-3 thousand versus 3-hundred events per burst, collected with the existing DAQ).

As the first stage of the upgrade program we made several refinements:

1. A new γ-spectrometer with 39 $\times$ 27=1052 lead glass counters with the 5 cm $\times$ 5 cm $\times$ 42 cm dimensions was installed in the setup instead of the old γ-spectrometer [12] (with 320 lead glass counters with the 10 cm $\times$ 10 cm $\times$ 38 cm dimensions and only 63 counters of the 5 cm $\times$ 5 cm $\times$ 38 cm size in the central part of the photon detector). A new γ-spectrometer is a modified version of the IHEP IGD γ-spectrometer which was used previously in the EGS experiment at CERN [29].

2. Four additional planes of the drift tubes [30] were installed between the multicell threshold Cherenkov counter and the γ-spectrometer (see layout of the SPHINX apparatus, Fig.3). In a modernized setup we removed the threshold

Cherenkov counter $\breve{C}_2$ because of a good identification capability of the RICH and $\breve{C}_1$ Cherenkov detector based system.

3. New trigger requirements made it possible to detect $\Lambda \to p\pi^-$ decays on the $L \approx 300$ cm decay path (instead of $L \approx 30$ cm in the previous runs).

As a result of this upgrade a detection efficiency and purity of the Λ events were significantly increased. Better photon identification in the new γ-spectrometer allows to reduce backgrounds due to hadron showers and lost photons. This is particularly important for identification of single photons (e.g., in the radiative $\Sigma^0 \to \Lambda\gamma$ decays). To illustrate these new features we present $\Lambda \to p\pi^-$ peak observed in the old and new $p + N \to \Lambda K^+ + N$, $\Lambda \to p\pi^-$ data (Figs.8, 9), as well as the identification of Σ^0 in the $p + N \to \Sigma^0 K^+ + N$, $\Sigma^0 \to \Lambda\gamma$ reaction (Figs.4d, 10). It is clear that with a partially upgraded SPHINX detector we can select reactions with Λ and Σ^0 hyperons production much more effectively.

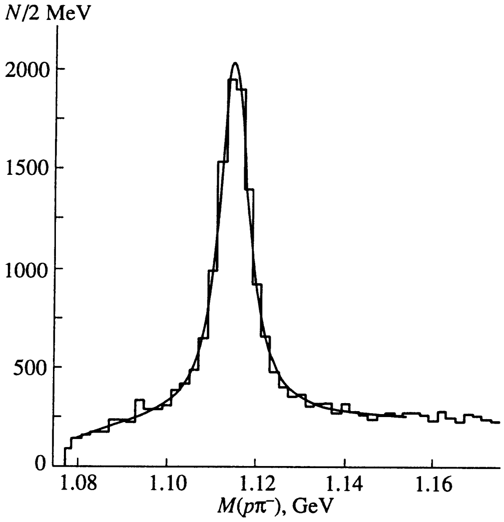

Figure 8: Selection of the reaction $p + N \to [\Lambda K^+] + N$ from the invariant mass spectrum of $(p\pi^-)$ produced in the reaction $p + N \to [p\pi^- K^+] + N$ (data were collected with an old version of the SPHINX detector with the $\Lambda \to p\pi^-$ decay path $L \simeq 30$ cm; it was impossible to resolve effectively the primary and secondary vertices).

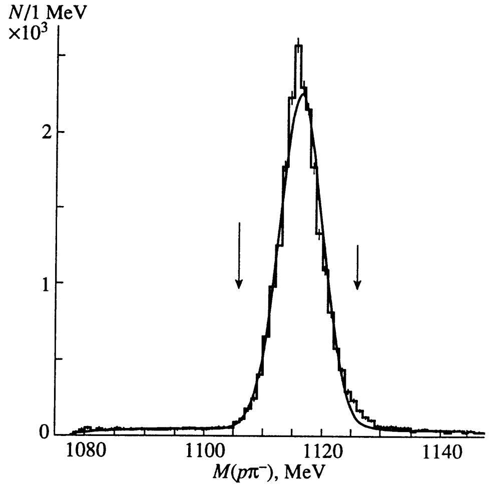

Figure 9: Selection of the reaction $p + N \to [\Lambda K^+] + N$ from the exclusive $p + N \to [p\pi^- K^+] + N$ data taken with the upgraded SPHINX detector with the $\Lambda \to p\pi^-$ decay path $L \approx 300$ cm which allowed for a reliable identification of Λ decay vertices. Background under Λ peak in the $M(p\pi^-)$ spectrum is significantly reduced comparing to that in Fig.8.

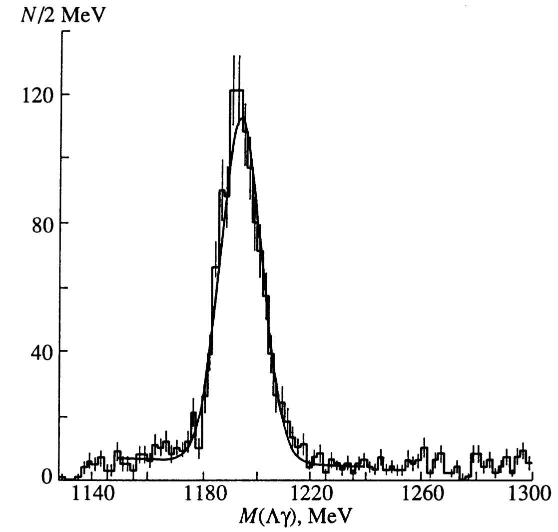

Figure 10: Selection of the reaction $p+N \to [\Sigma^0 K^+] + N$ from the invariant mass spectrum of the $(\Lambda\gamma)$ system produced in the reaction $p+N \to \Lambda\gamma K^+ + N$. Data were taken with the upgraded SPHINX detector with an improved identification of $\Lambda \to p\pi^-$ decay and single photon in the new γ-spectrometer. Background under Σ^0 peak in $M(\Lambda\gamma)$ is significantly reduced compared to that in Fig.4d.

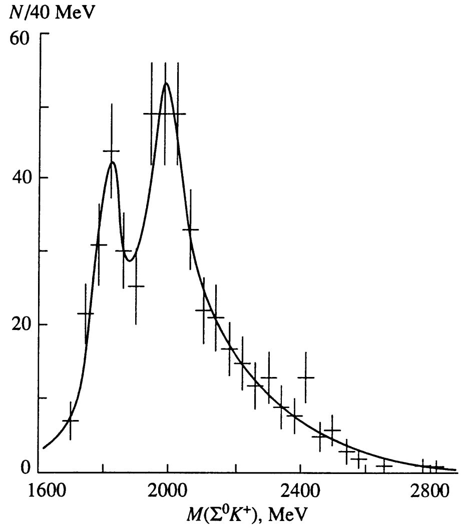

Figure 11: Invariant mass spectrum of the $(\Sigma^0 K^+)$ system produced in the coherent reaction (16) in a special run of the upgraded SPHINX detector ($P_T^2 < 0.1$ GeV^2). Because of the low background under Σ^0-peak in Fig.10 no background subtraction was done in the $M(\Sigma^0 K^+)$ spectrum. The results on the $(\Sigma^0 K^+)$ mass spectrum from this run are in a good agreement with the old data [18, 19, 20], see Fig.7.

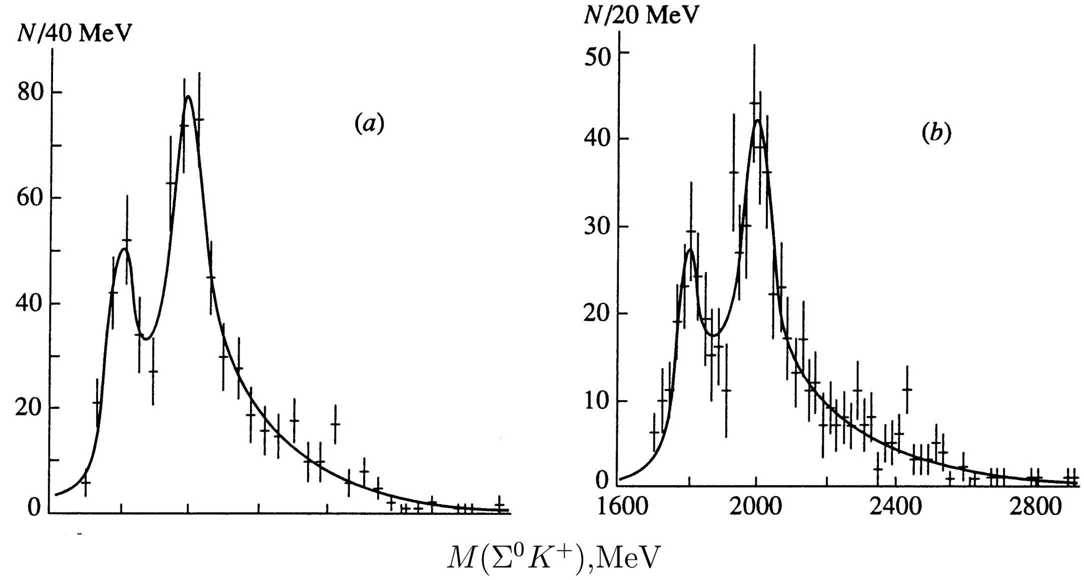

Figure 12: Combined mass spectrum $M(\Sigma^0 K^+)$ for the data in Figs.7b and 11: a) 40 MeV mass bin; parameters of the $X(2000)$ peak are $M = 1995 \pm 7$ MeV and $\Gamma = 103 \pm 19$ MeV; b) 20 MeV mass bin; parameters of the $X(2000)$ peak are $M = 2001 \pm 7$ MeV and $\Gamma = 88 \pm 25$ MeV.

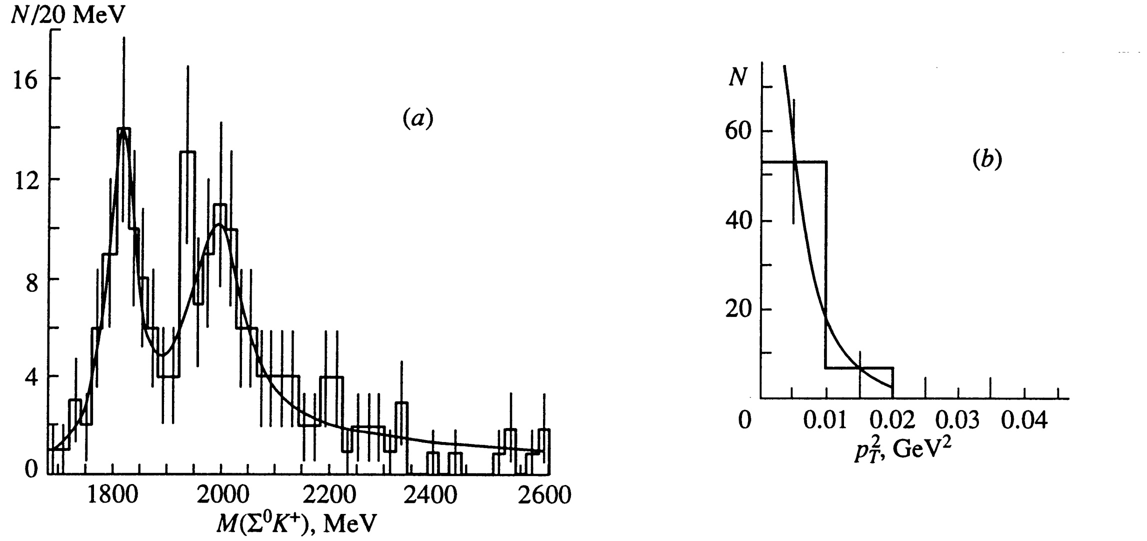

Figure 13: Study of a narrow threshold structure in the mass spectrum of the $(\Sigma^0 K^+)$ system produced in the coherent reaction (16) (data taken with the upgraded SPHINX setup): a) invariant mass spectrum $M(\Sigma^0 K^+)$ for $P_T^2 < 0.01$ GeV^2; a threshold structure with $M = 1812 \pm 7$ MeV and $\Gamma = 56 \pm 16$ MeV is clearly seen; b) a P_T^2 dependence for this threshold structure production.

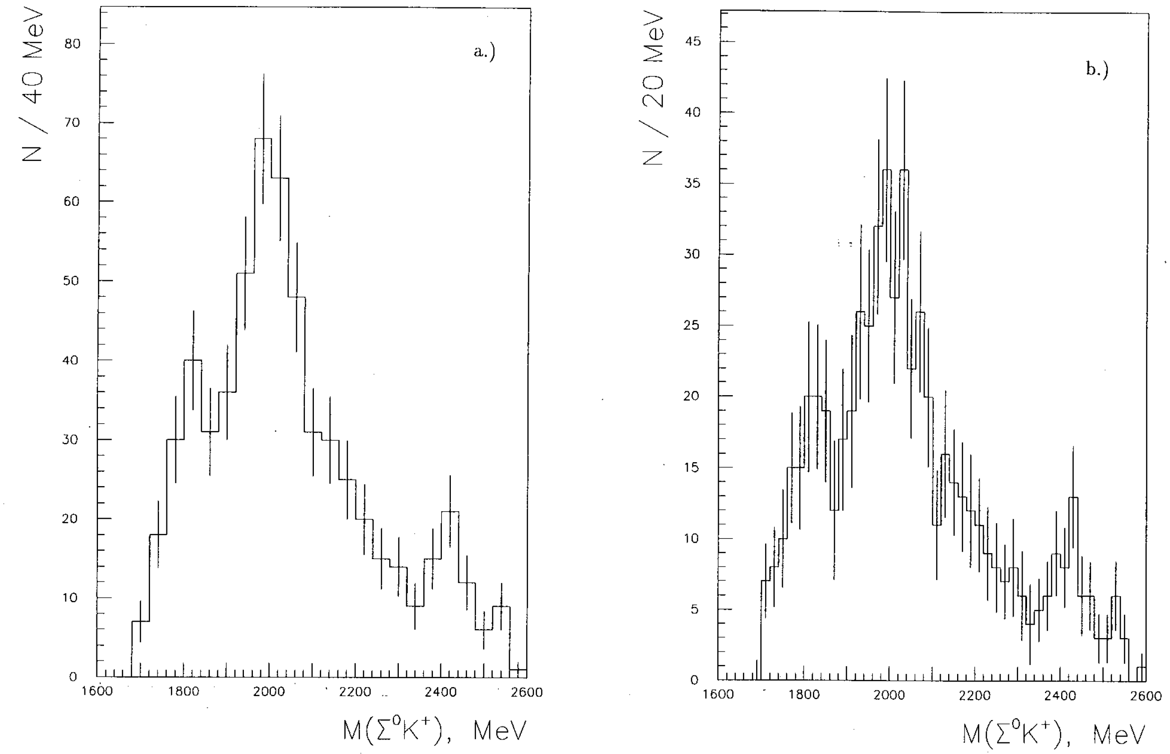

Figure 14: a,b) The same $M(\Sigma^0 K^+)$ combined mass spectra as on Fig. 12 a,b, but with modified coherent cut $0.01 < P_T^2 < 0.1$ GeV^2 (to reduce the influence of the threshold structure of Fig.13).

6. New $p + C \to [\Sigma^0 K^+] + C$ data from a special run with the partially upgraded SPHINX spectrometer[21]

The production of the $(\Sigma^0 K^+)$ system in the $p + N \to [\Lambda\gamma K^+] + N$ reaction was clearly identified (see Fig.10) with the partially upgraded SPHINX spectrometer in a special test run. Background under the Σ^0 peak is small, which simplifies selection of the reactions under study since there is no need for background subtraction in this case. To select a coherent reaction (6) we used the "loose" cut on the transverse momentum $P_T^2 < 0.1$ GeV^2, as it was done in the previous analysis. The invariant mass spectrum $M(\Sigma^0 K^+)$ for this coherent reaction from new data is presented in Fig.11. This spectrum is in a good agreement with that in Fig.7: there is again a clear $X(2000)$ peak and a threshold structure with $M \sim 1800$ MeV. The combined spectrum from the old data (Fig.7b) and new data (Fig.11) is presented in Fig.12. A sum of the spectra in Fig.7a (no background subtraction) and Fig.11 gives a similar result. The average parameters of the $X(2000)$ structure obtained from the different combined $M(\Sigma^0 K^+)$ invariant mass spectra are:

$$\left.\begin{array}{l} M = 1996 \pm 7\,\text{MeV}; \\ \Gamma = 99 \pm 21\,\text{MeV}; \\ \text{statistical significance of the peak} \ > \ 10 \text{ s.d.} \end{array}\right\} \quad (17)$$

It is important to mention that the old and new data from the coherent diffractive reaction (6) were obtained under different experimental conditions, with significant modifications in the detector, different background and systematics. Nevertheless, the $\Sigma^0 K^+$ invariant mass spectra from two runs are in a good agreement which makes them more reliable.

An increased statistics allowed for a detailed study of the effect of a "tight" P_T^2 cut on the shape of the $\Sigma^0 K^+$ mass spectrum. The tight cut reduces a noncoherent background and therefore enhances the coherent process (6). As was shown before [18, 19] the parameters of the $X(2000)$ peak are not affected by the tight P_T^2 cut. However, we quite unexpectedly found a strong influence of this cut on the shape of the threshold structure at 1800 MeV. As is seen from Fig.13, this structure is produced only at very small P_T^2. For $P_T^2 < 0.01$ GeV^2 it is clearly observed and has the parameters.

$$\left.\begin{array}{l} M = 1812 \pm 7\,\text{MeV}; \\ \Gamma = 56 \pm 16\,\text{MeV}. \end{array}\right\} \quad (18)$$

These peculiar properties of the threshold structure are not well understood yet and require a further study with larger statistics and under different experimental conditions (e.g. in the coherent processes with heavier nuclei).

It is possible to modify P_T cut for the events of coherent reaction (6) to suppress the influence of the threshold structure and to observe the $X(2000)$ peak in more clear conditions.

This new transverse momentum cut is: $0.01 < P_T^2 < 0.1$ GeV^2. The corresponding results in combined $\Sigma^0 K^+$ invariant mass spectrum are presented in Fig.14.

7. First data on the proton diffractive-like production in a nonperipheral domain [20,21]

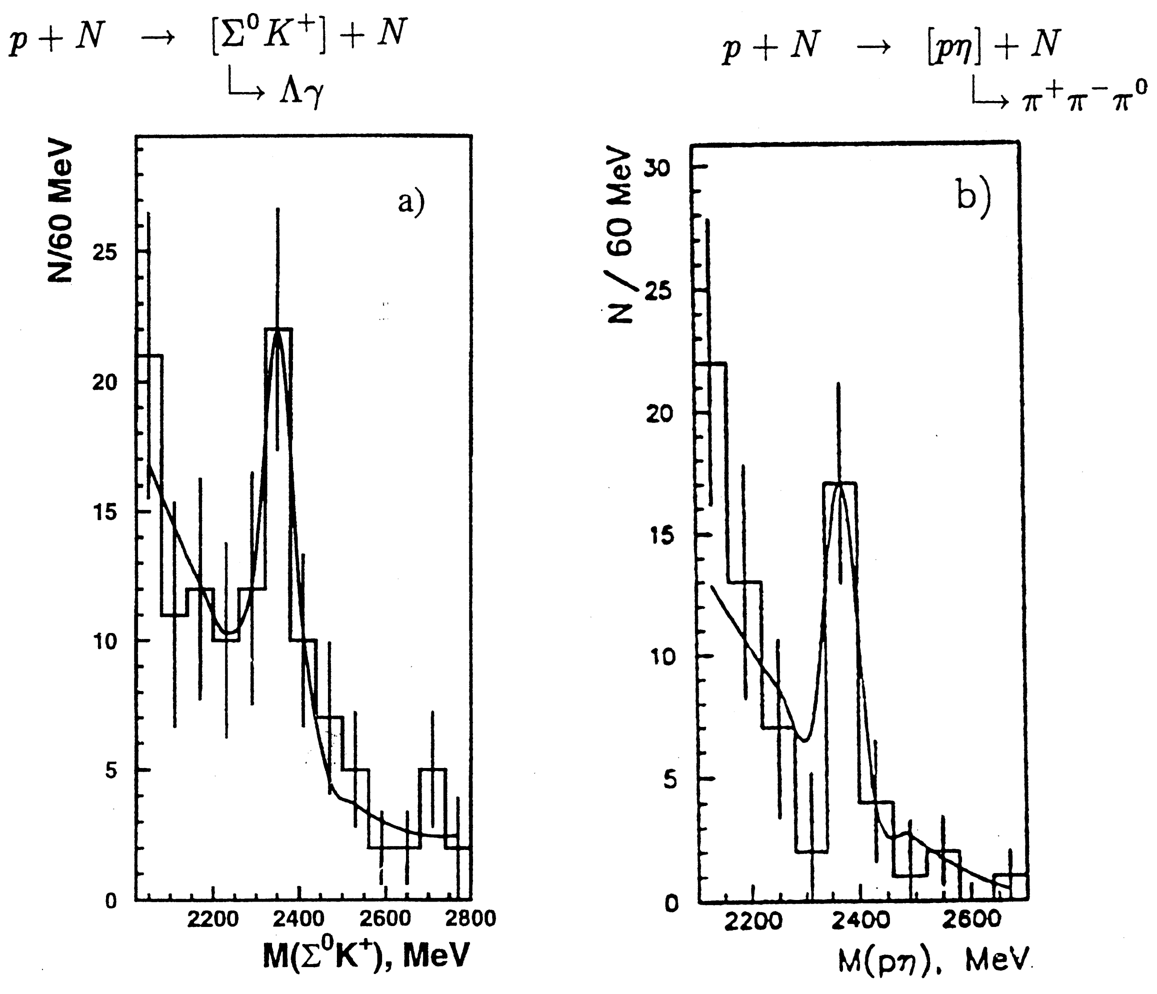

Figure 15: a) Invariant mass spectrum of the $(\Sigma^0 K^+)$ system produced in the reaction $p + N \rightarrow [\Sigma^0 K^+] + N$ (10) at $P_T^2 > 0.3$ GeV^2 (combined data from the old and new runs). b) Invariant mass spectrum of the $(p\eta)$ system produced in the reaction $p + N \rightarrow [p\eta] + N$ (31) at $P_T^2 > 0.3$ GeV^2 (old data, see [20]). A narrow structure with $M \sim 2350$ MeV and $\Gamma \sim 60$ MeV in the non-peripheral region of (10) and (31) is seen in these mass spectra.

As was discussed above, coherent diffractive production reactions seem to be quite promising processes to search for exotic hadrons, but, certainly, not the only ones. For instance, a nonperipheral production can be the most effective way to look for certain exotic states especially for those that are formed at short ranges. In this case the best conditions for the exotic hadron production are achieved at higher transverse momenta ($P_T^2 > 0.3 - 0.5$ GeV^2), where the background from peripheral processes is strongly suppressed. For instance, non-typically narrow meson states $X(1740) \to \eta\eta$ [31] and $X(1910) \to \eta\eta'$ [32] were observed in the study of the charge-exchange reactions $\pi^- p \to [\eta\eta] + \Delta^0$ and $\pi^- p \to [\eta\eta'] + n$, after the selection of events with $P_T^2 \geq 0.3$ GeV^2. These anomalous states are good candidates for cryptoexotic mesons. A mechanism of multiple rescattering with the Pomeron exchange (a gluon rich process) may explain the $X(1740)$ and $X(1910)$ production [33].

Searches for new baryons in the proton -induced diffractive-like reactions at high P_T^2 also seem to be quite promising [20,21]. Here we present the first (very preliminary) results on the invariant mass spectra of the $(\Sigma^0 K^+)$ and $(p\eta)$ systems produced in the reactions

$$\begin{aligned} p + N \quad \to \quad & [\Sigma^0 K^+] + N \\ & \hookrightarrow \Lambda\gamma \end{aligned} \tag{19}$$

and

$$\begin{aligned} p + N \quad \to \quad & [p\eta] + N \\ & \quad \hookrightarrow \pi^+\pi^-\pi^0 \end{aligned} \tag{20}$$

with $P_T^2 > 0.3$ GeV^2 (see Ref.[20] for the latter process). Combined data for the reaction (19) from the old and new runs are shown in Fig.15a. The data from the old run for the reaction (20) are shown in Fig. 15b. Despite the limited statistics, a structure with the mass $M \approx 2350$ MeV and the width $\Gamma \sim 60$ MeV can be clearly seen in these two mass spectra. They require a further study in future experiments with large statistics.

8. Reaction $p+N \to (\Sigma^0\pi^0)K^+ + N$ and perspectives for a study of Λ^* hyperon resonances

Diffractive reactions of $p + N \to [Y^* K^+] + N$ type with hyperon and kaon production can be also used to probe the excited hyperon states Y^*. For example, we present here some results of the SPHINX Collaboration on the study of $\Sigma^0\pi^0$ system in the diffractive reaction

$$\begin{aligned} p + N \quad \to \quad & (\Sigma^0 \pi^0) K^+ + N. \\ & \quad\; \hookrightarrow \gamma\gamma \\ & \hookrightarrow \Lambda\gamma \end{aligned} \tag{21}$$

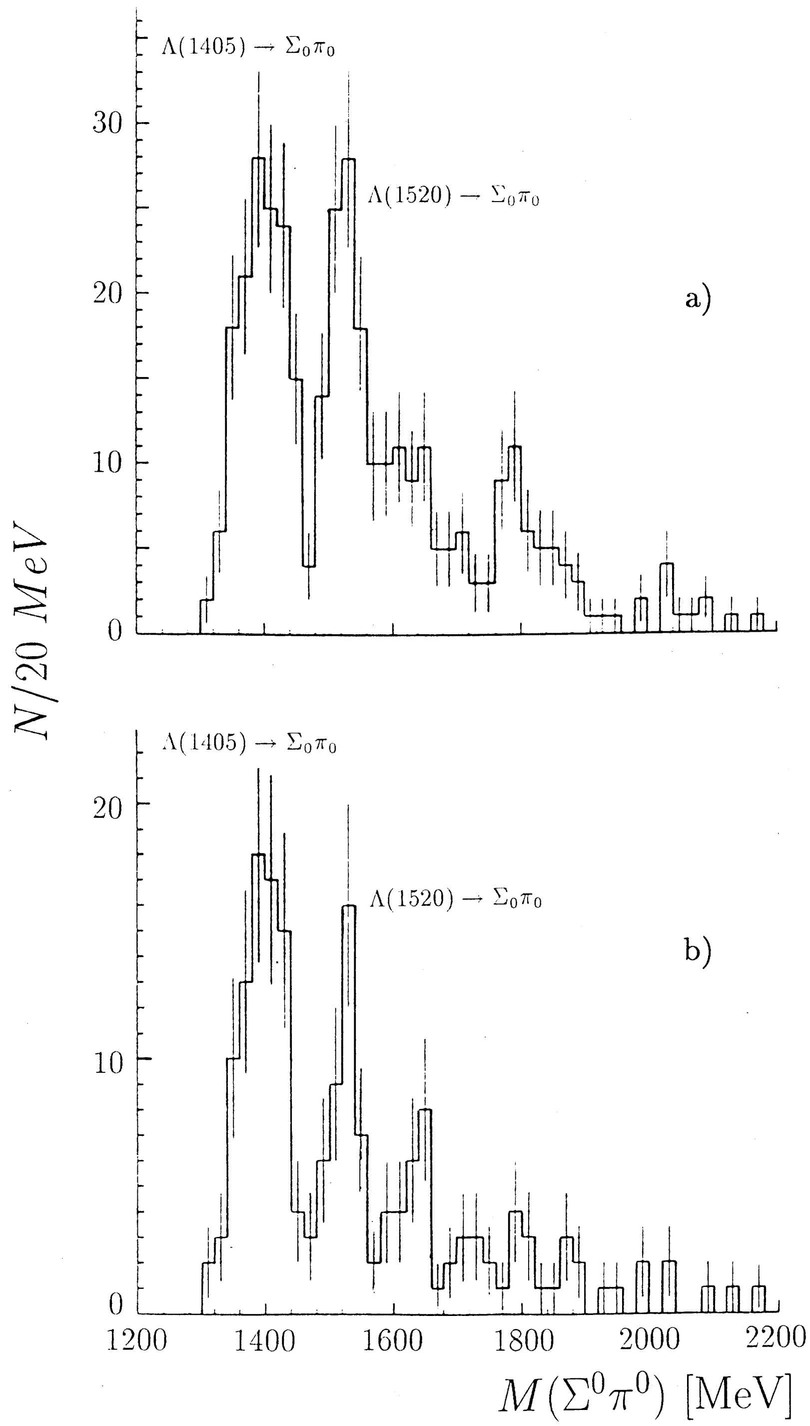

Figure 16: The mass spectra $M(\Sigma^0\pi^0)$ for the reaction $p + N \to (\Sigma^0\pi^0)K^+ + N$: a) for all P_T^2; b) for $P_T^2 < 0.075$ GeV^2 (coherent production).

The $(\Sigma^0\pi^0)$ - system can be characterized by the isotopic spin values $I = 0$ or $I = 2$. But in the proton diffractive process (21) with the Pomeron exchange only isoscalar $(\Sigma^0\pi^0)$ - system can be produced (because the primary proton and secondary kaon are isospinors). Thus, reaction (21) offers a possibility to study isoscalar Λ^* hyperon resonances in the $\Sigma^0\pi^0$ system in pure conditions, without the influence of isovector Σ^* background. As is clear from PDG [34], the properties of the most of Λ^* states are poorly understood now and new data for these states are quite desirable. The first results of the SPHINX experiment for the invariant mass spectra $M(\Sigma^0\pi^0)$ are presented in Fig.16 (these are obtained in the old run with a small decay path for $\Lambda \to p\pi^-$ and with limited statistics). One might expect from this figure that in new measurement with enlarged statistics it would be possible to obtain a rich data for several Λ^* states. In particular, it seems quite interesting to perform a detailed study of the shape for $\Lambda(1405)$ peak in this process. There were some previous evidences of an anomalous (non Breit – Wigner) behavior of mass spectra for $\Lambda(1405)$ hyperon [34-36]. Such non-Breit – Wigner form of $\Lambda(1405)$ peak can be caused by possible exotic nature of this hyperon (bound K^-p state?).

9. Conclusion

Let us summarize the main results of the SPHINX Collaboration presented above:

1. The extensive research program of studying the diffractive production reactions on the proton beam with $E_p = 70$ GeV is carried out in the experiments at the SPHINX setup [2, 12-22]. The main aims of this program are the searches for cryptoexotic baryons with hidden strangeness $|uuds\bar{s}>$. Only part of these experiments is discussed here.

2. In our previous measurements [18-20] the coherent diffractive production reactions $p + C \to [\Sigma(1385)^0K^+] + C$ and $p + C \to [\Sigma^0K^+] + C$ were investigated. The evidences for new baryon states were obtained in the study of hyperon-kaon effective mass spectra in these two reactions: $X(2050) \to \Sigma(1385)^0K^+$ with mass $M = (2052 \pm 6)$ MeV and width $\Gamma = (35^{+22}_{-35})$ MeV and $X(2000) \to \Sigma^0K^+$ with $M = (1997 \pm 6)$ MeV and $\Gamma = (91 \pm 17)$ MeV. The unusual dynamical feature of these massive states (relatively narrow decay width, anomalously large branching ratios for the decays with strange particle emission) make them serious candidates for cryptoexotic pentaquark baryons with hidden strangeness. In spite of significant statistical confidence of the observation of new states we considered these results as preliminary, which must be confirmed in further measurements with increased statistics.

3. The first results on new test run with the partly modified SPHINX setup (with a new γ-spectrometer and with better possibilities for $\Lambda \to p\pi^-$ identification) for the coherent reaction $p + C \to [\Sigma^0K^+] + C$ are present now [21]. These

results are in a very good agreement with our previous data for this reaction. In the combined effective mass spectrum $M(\Sigma^0 K^+)$, besides some threshold structure with $M \sim 1800$ MeV, a strong peak $X(2000) \to \Sigma^0 K^+$ is dominated. The average mass and width of this peak are $M = 1996 \pm 7$ MeV and $\Gamma = 99 \pm 21$ MeV. Because of the significant modification of the equipment, the good agreement between previous and new data gave us an additional confidence for the real existence of $X(2000)$ anomalous baryon state – the candidate for the baryon exotics $|uuds\bar{s}>$.

4. A narrow threshold structure with $M \sim 1810$ MeV and $\Gamma \sim 60$ MeV was observed in the $M(\Sigma^0 K^+)$ mass spectrum, as it was stated before. It was found that this structure is produced practically only in the region of very small $P_T^2 (\leq 0.01 \div 0.02 \text{ GeV}^2)$ where it is seen quit clearly.

5. The first data in nonperipheral domain (at $P_T^2 > 0.3$ GeV^2) were obtained in the reactions $p + N \to [\Sigma^0 K^+] + N$ and $p + N \to [p\eta] + N$. In both reactions there is evidence for a narrow enhancement with $M \sim 2350$ MeV and $\Gamma \leq 60$ MeV [20, 21].

6. A further study of Λ^* hyperon isoscalar resonances might be performed in the $[\Sigma^0 \pi^0]$ system (to be produced in the diffractive reaction $p+N \to [\Sigma^0\pi^0]K^+N$).

Further development of experimental program of the search for exotic baryon is expected with future measurements of the SPHINX Collaboration. We hope to obtain a significantly larger statistics for these processes in the next runs with a totally upgraded SPHINX setup. This upgrade is succesfully completed now and new measurements on the beam are underway.

References

[1] Landsberg L.G. Surveys in High Energy Phys., 1992, v.6, p.257;

[2] Landsberg L.G. Yad Fiz., 1994, v.57, p.47; Landsberg L.G. UFN, 1994, v.164, p.1129.

[3] Peters K. Proc. of the Second Biennial Conf. on Low Energy Antiproton Phys. (LEAP-92), Courmayeur, Aosta Valley, Italy, September 14-19, 1992 (Ed C.Guaraldo et al.), Nucl. Phys., 1993, v.A558, p.92.

[4] Dover C.B. LEAP-92 Summary talk, Ibid. Nucl. Phys., 1993, v. A558, p.721.

[5] Amsler C. Rapporter talk, Proc. of 27 Intern. Confer. on High Ehergy Phys. (ICHER), Glasqow, Scotland, July 1994.

[6] Close F.E. Preprint RAL-87-072, Chilton, 1987.

[7] Blum P. Int. Journ. of Mod. Phys., 1996, v. 11A, p. 3003.

[8] Hirose T. et al. Nuov. Cim., 1979, v.50A, p.120; Fucunage C. at al. Nuov. Cim., 1980, v.58, p.199.

[9] Amirzadeh J. et al. Phys. Lett., 1979, v. 89B, p.125.

[10] Aleev A.N. et al. Z. Phys., 1984, v. 25C, p.205.

[11] Karnakov V.M. et al. Phys. Lett., 1991, v. 281B, p. 148.

[12] Vavilov D.V. et al. Yad. Fiz., 1994, v.57, p.241; Balatz M.Ya. et al. Z.Phys., 1994, v. 61C, p.220.

[13] Balatz M.Ya et al. Z.Phys., 1994, v. 61C, p.399.

[14] Vavilov D.V. et al. Yad. Fiz., 1994, v.57, p.253.

[15] Landsberg L.G. et al. Proc. of "Hadron-93", Villa Olmo, Como, June 21-25, 1993 (ed. Bressani T. et al.), Nuov. Cim., 1994, v. 107A, p. 2441.

[16] Kurshetsov V.F., Landsberg L.G. Yad. Fiz., 1994, v. 57, p. 2030.

[17] Vavilov D.V. et al. Yad. Fiz., 1994, v. 57, p. 1449.

[18] Vavilov D.V. et al. Yad. Fiz., 1995, v. 58, p. 1426.

[19] Golovkin S.V. et al. Z. Phys., 1995, v. 68C, p. 585.

[20] Golovkin S.V. et al. Yad.Fiz., 1996, v. 59, p. 1395

[21] Bezzubov V.A. et al. Yad. Fiz., 1996, v. 59(in press)

[22] Vavilov D.V. et al. Yad. Fiz., 1994, v.57, p. 2046.

[23] Chan Hong-Mo, Hogaasen H. Phys. Lett., 1977, v. 72B, p. 121; Chan Hong-Mo et al. Phys. Lett., 1978, v. 76B, p. 634.

[24] Hogaasen H., Sorba P. Nucl. Phys., 1978, v. 145B, p. 119; Hogaasen H., Sorba P. Invited Talk at Conf. on Hadron Interastions at High Energy, Marseiler, June, 1978.

[25] De Crombrugghe M. et al. Nucl. Phys., 1979, v. 156B, p.347.

[26] Chan Hong-Mo, S.T. Tsou. Nucl. Phys., 1977, v. 118B, p. 413.

[27] Landsberg L.G. UFN, 1990, v. 160, p. 1.

[28] Bellini G. et al. Nuov. Cim., 1984, v.79A, p. 282.

[29] Powell B. et al. Nucl. Instr. Meth., 1982, v. 198, p. 217.

[30] Denisov D.S., Musienko Yu. V. Preprint IHEP 85-72, Serpukhov, 1985; Denisov D.S. et al. Preprint IHEP 86-179, Serpukhov, 1986.

[31] Alde D. et al. Phys. Lett., 1986, v. 182B, p.105; Alde D. et al. Yad. Fiz., 1991, v. 54, p. 745; Phys. Lett., 1992, v. 276B, p. 457.

[32] Alde D. et al. Phys. Lett., 1989, v. 216B, p.447; Alde D. et al. Yad. Fiz., 1991, v. 54, p. 751; Phys. Lett., 1992, v. 276B, p. 375.

[33] Gershtein S.S. Proc. of the Third Intern. Conf. on Hadron Spectroscopy ("Hadron-89"), Ajaccio, Corsica, September 23-27, 1989 (ed. F.Binon et al.), Paris, 1989, p.175.

[34] Barnett R.M. et al. (PDG), Phys. Rev., 1996, v. 54D, p. 1; Montanet L. et al. (PDG) Phys. Rev., 1994, v. 80D, p.1173; Betsch G.I. et al. (PDG) Phys. Lett., 1990, v. 239B, p.1.

[35] Hemingway R.J. Nucl. Phys., 1985, v. 253B, p. 742.

[36] Barrett R.C. Nuov. Cim., 1989, v. 102A, p. 179.